Indian J. Phys. **76B** (3), 235–249 (2002)

REVIEW

I J P B
— an international journal

Lightning generated ELF, VLF, optical waves and their diagnostic features

R P Singh*, R P Patel and Ashok K Singh
Atmospheric Research Laboratory, Department of Physics, Banaras Hindu University, Varanasi-221 005, Uttar Pradesh, India
and
I M L Das
Department of Physics, Allahabad University, Allahabad-211 002, Uttar Pradesh, India
E-mail : rampal@banaras.ernet.in

Received 16 July 2001, accepted 8 February 2002

Abstract Recent observations of optical phenomena above an active lightning discharge such as red sprites, blue jets, blue starters and elves have refocused interest in this field and its consequences. It is argued that during lightning discharge ELF, VLF and optical emissions are generated. Analyzing the recorded data it is clearly shown that intense ELF generation from positive cloud to ground lightning discharge is an indication of the presence of red sprite. Daytime observation of red sprite is difficult and hence ELF waves can work as an indicator.

The diagnostic features of ELF and VLF waves are also discussed and interesting results based on the analysis of whistlers recorded at Indian stations are presented. Recently, association of VLF waves with Earthquakes and red sprites are reported We have briefly summarized some results related with these phenomena.

Keywords : ELF, VLF waves, optical emissions, lightning discharge, diagnostics.

PACS Nos. : 94.30.Tg, 92.60.Pa, 91.30.Px

Plan of the Article

1. Introduction

The lightning is known to arise from Cloud to Ground (CG), Cloud to Cloud (CC) and Intra-Cloud (IC) electrical discharges. The observation of electromagnetic phenomena associated with lightning helped to a large extent in its understanding. The radiation of electromagnetic waves from lightning discharge can be considered as radiation from electric dipole antenna. The CG radiate electromagnetic waves like a vertical dipole antenna where as CC and IC radiate electromagnetic waves like horizontal dipole. Some times they may be considered as a dipole aligned at certain angle from the vertical. As a result of lightning, energized charge particle beam is set up which is known to radiate wide spectrum of electromagnetic waves : optical emissions, X-rays and gamma-rays [1–3]. The microprocesses in the CG, IC and CC-discharges are not well understood and efforts are being made to understand the involved physical processes. The complex electrodynamic properties of the atmosphere influence the excitation and propagation of electromagnetic signal generated by lightning discharges and give rise to a diversity of the typical signal wave forms and amplitudes in the various space-time domains.

*Corresponding Author

This causes difficulties and controversies in the interpretation of experimental data.

In this review, we shall be discussing extremely low frequency (ELF) and very low frequency (VLF) waves in electromagnetic wave phenomena and sprites in the optical radiation. Lightning discharges excite the natural cavity formed by the surface of the Earth and the lower ionosphere, which oscillates at discrete frequencies known as Schumann resonance frequencies. The eigen frequencies of oscillations are 7.8, 14.0, 20.0, 26.0, 33.0, 39.0, 45.0 Hz and amplitude varies between 100 and 200 $\mu Vm^{-1}Hz^{-1}$ [4]. These waves are used to monitor thunderstorms, sprites and total sprite luminosity.

Atmospherics, whistlers and VLF emissions are a group of complex and fascinating natural wave phenomena generated during lightning discharges, which were the first to be observed amongst plasma waves from space. The part of VLF wave energy from lightning discharge propagating upward is trapped in the Earth-ionosphere wave-guide and may echo back and forth between the boundaries of the wave-guide many times before disappearing into the back ground noise. The signal having very little dispersion is known as atmospherics or sferics. It has been used to study ionization at the lower edge of the ionosphere [5,6]. The part of VLF wave energy which is not reflected back from the lower edge of the ionosphere, penetrate the ionosphere and propagate along dipolar geomagnetic field lines either in ducted or non-ducted mode. These waves can propagate back and forth along the field lines without much attenuation. The presence of ionization along with magnetic field produces dispersion in the VLF wave. Usually, high frequency component travels faster as compared to low frequencies and signal is termed as whistler. The spectrum could be very sharp or diffused depending upon the nature of the duct through which it has propagated. Whistler has been used as a potential diagnostic tool [7,8] of the magnetosphere. Plasma parameters such as density, large scale electric fields and electron temperature are determined from the dispersion analysis of whistler waves. Ion compositions are derived from hydromagnetic whistlers or ion cyclotron waves [9]. Whistler mode waves have also been used to diagnose magnetic fields and particles in the solar corona [10]. Plasma parameters in the outer magnetosphere can be studied by analyzing VLF whistlers observed in the outer magnetosphere [11]. Lightning excites whistlers not only in Earth's magnetosphere but also on Jupiter [12], Neptune [13,14] and Venus [15], although the latter observations are still being debated [16,17].

Earlier, the region above thunder storm was considered to be passive, doing little more than to allow radio waves through to the ionosphere and pass the thunderstorm (vertical) currents that help to maintain the electrification of the fair weather atmosphere through the thunderstorm driven global electric circuit. This region gained importance because of the observation of transient optical phenomena lasting less than 30 seconds. These events are red sprites, blue jets and blue starters [2]. Fishman *et al* [1] have demonstrated the existence of a number of gamma-ray events associated with lightning discharge. Following the experimental break through, there have been many suggestions about the generation and propagation mechanism of these signals [18].

In this paper an attempt has been made to summarize the available information about the ELF and VLF waves, and optical emissions. Emphasis is mostly on the diagnostic features of these radiations caused by lightning discharges.

2. ELF waves/Schumann resonances

The active research in the entire band of ELF propagation was stimulated because of US Navy's interest in investigating this band for possible application in submarine communications [19]. Williams [20] has discussed novel application of Schumann resonances to Earth system studies. Schumann resonances are the eigen-frequencies of the Earth-ionosphere cavity oscillations excited by global lightning activity over the frequency range 6 to 50 Hz [21]. The principal features are summarized below

	Property	Vertical electric fields	Horizontal magnetic fields
(i)	Eigen frequencies $f_n < 50$ Hz	7.8, 14, 20, 26, 33, 39, 45 Hz	7.8, 14, 20, 26, 33, 39, 45 Hz
(ii)	Diurnal variation of f_n	± 0.5 Hz	± 0.5 Hz
(iii)	Amplitude	~100–200 $\mu Vm^{-1}Hz^{-1/2}$	0.5–1 $pTHz^{-1/2}$
(iv)	Diurnal amplitude variation	± 50–100 $\mu Vm^{-1}Hz^{-1/2}$	± 0.25–0.5 $pTHz^{-1/2}$
(v)	Maximum intensity period (western hemisphere)	2000–2200 UT	2000–2200 UT
(vi)	Polarization	Linear (vertical)	Linear (elliptical)
(vii)	Primary source of interference	Power lines, acoustic noise, blowing dust, rain *etc*	Power lines, acoustic noise, movement of vehicles, magnetic materials *etc*

Cloud to ground discharges are believed to be the principal excitation sources of Schumann resonance. Uman [22] argued that global average discharge rates of 100 sec^{-1} with peak currents of the order of 20–30 kA for strokes of average lengths of 3 to 5 km, are sufficient to excite the Earth-ionosphere cavity to the observed level of intensities of both electric and magnetic field spectra. The diurnal intensity profiles are similar for both electric and magnetic field spectra. Usually, Schumann resonance

intensities undergo a quasi-periodic diurnal modulation in both the vertical electric field and horizontal magnetic field intensities. Sentmann [23] has discussed day to day variations in the diurnal profile in terms of variability in the totality of the global lightning source functions. The contribution from lightning over the oceans is relatively small. Diurnal profiles simultaneously recorded at widely separated locations show striking differences. If correction to local time effects is taken into account (assuming uniform distribution of Schumann resonance energy in the cavity and conservation of wave energy), then the power spectra recorded at two different stations become identical. This shows that Schumann resonance energy is uniformly distributed throughout the Earth-ionosphere cavity, eventhough lightning discharge is not uniformly distributed over the whole globe. Thus, Schumann resonances may be considered as a unique signature of global lightning and it can be used to monitor global lightning activity [24,25]. Williams [20] demonstrated a clear annual correlation over a six year span between the variation of the first Schumann resonance mode intensity (horizontal magnetic field component) and the tropical temperature exhibiting the fact that it can be used as a global tropical thermometer. Additional observations and theoretical work are needed in several key areas to establish the strength of the thunderstorm-resonance link. Further, large scale distortions in the upper boundary of the Earth-ionosphere cavity may also produce corresponding effects on Schumann resonances. An assessment is required both theoretically and observationally, of the effect of such ionospheric perturbations on the resonances before it can be used for proper diagnostic purposes.

A part from cloud to ground discharge, the vertical current component of intra-cloud and inter-cloud discharges could also excite the Earth-ionosphere cavity. The fluctuating current in the auroral electrojet with total current ~10^6 A flowing within the upper boundary of the cavity at altitudes of 100 km and modulated by magnetospheric Alfvén waves could also excite the cavity [26]. Reising *et al* [27] has indicated that the resultant electrical current associated with optical flashes between the cloud tops and ionosphere could constitute a potential electric dipole excitation source of the Earth-ionosphere cavity. High-resolution photometer measurements and ELF measurements demonstrate the simultaneity of sprite luminosity and the second ELF pulse [28]. Fullekrug and Reising [29] have studied the distribution of first return stroke peak current with lightning flashes recorded by National Lightning Detection Network on August 1, 1996 and have shown that most of the lightning discharges are associated with negative cloud to ground currents. The data is shown in Figure 1. The peak occurrence rate corresponds to currents −10 to −15 kA. Only a small number of discharges have positive cloud to ground currents. The association of Earth-ionosphere cavity resonance with lightning current is shown in Figure 2. It is seen from the

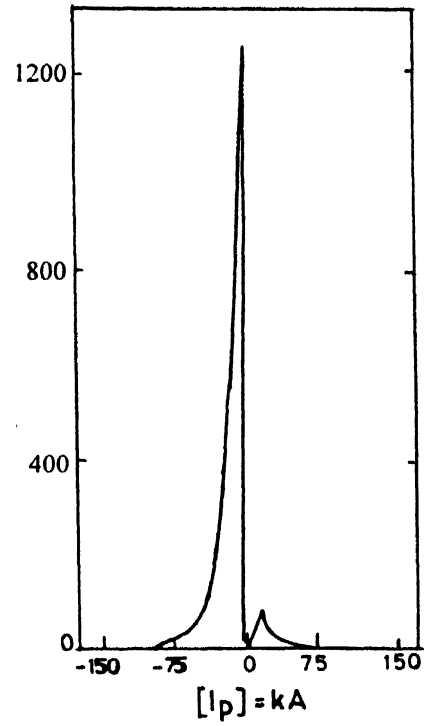

Figure 1. Distribution of lightning flashes as a function peak current during lightning discharge as recorded by NLDN on August 1, 1996.

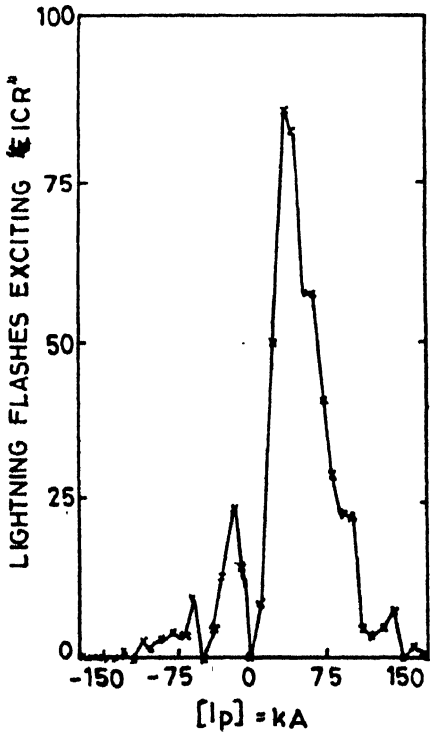

Figure 2. Distribution of lightning flashes exciting Earth-Ionosphere Cavity Resonances as a function of peak current during return stroke.

figure that large number of cavity resonances are excited by positive cloud to ground currents ~20 – 70 kA. Only less than the one-third events are associated with negative cloud to ground discharges. Similar result was reported by [29].

In Figure 3, we have plotted sprite associated lightning discharges as a function of peak current. Invariably, the number of discharges decreases as the peak current increases. It is noted that for peak current less than 50 kA, about 20% of the discharges are associated with sprites. As the peak current increases, the occurrence percentage of sprite increases. For example, the occurrence percentage of sprite rises to about 50% when peak current is less than 70 kA.

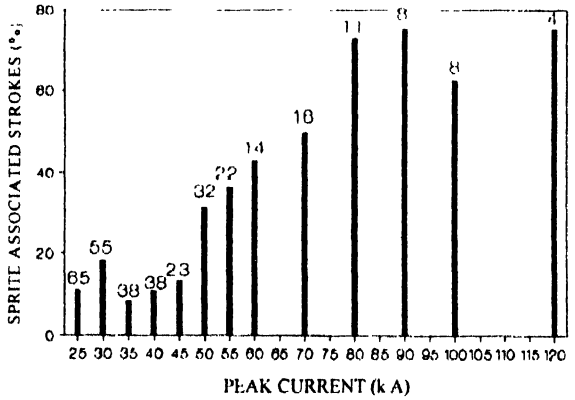

Figure 3. Distribution of sprite associated lightning discharge as a function of peak current. The number of events associated with each peak current is shown at the top of the vertical line inside the figure. The total number of events is 334.

For higher peak current (>80 kA) sprite associated strokes are greater than 70%. Sentmann *et al* [4] have also shown association of red sprite with strong positive cloud to ground discharges. It is also noted that large currents are associated with the excitation of Earth-ionosphere cavity resonance (EICR). Thus, it is seen that a lightning discharge occurring with large positive cloud to ground current is associated with both the EICR and optical transient phenomena such as red sprite. This shows that the large discharge current (>50 kA) may be responsible for the excitation of both EICR and optical phenomena. The monitoring of EICR on the Earth surface is easier and it can be used as an indicator of red sprite. Based on simultaneous detection of discrete excitation of EICR at two or more stations, we can predict the location of lightning discharge which may be associated with sprite. It should be noted that during daytime in the presence of intense sunlight, detection of optical transient phenomena becomes difficult whereas detection of EICR is simple and easy. Hence, EICR can be used as a tool to indicate the presence of transient optical emissions.

Figure 4 shows distribution of sprite associated sferics as a function of ELF sferics energy for the same number of flashes as shown in Figure 3. The number of events in each energy band are shown in the figure (total events = 334). In

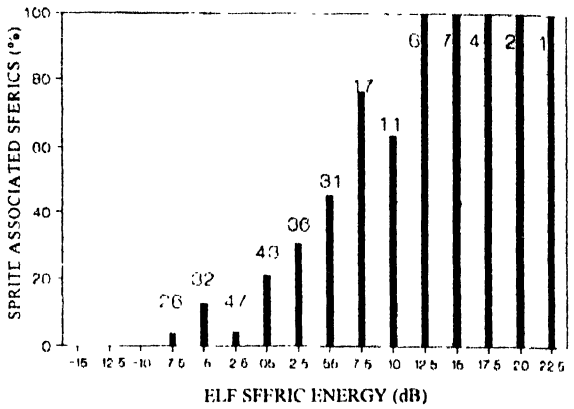

Figure 4. Distribution of sprite associated sferics as a function of ELF sferic energy in dB. Out of 334 event analyzed only 263 events were associated with sprites.

this diagram, 0 dB or base power is taken as 0.057 $(nT)^2$. The mean value of ELF sferic's energy is 0.5 dB. It is noted that about 20% sprites are associated when individual ELF energy equals to mean value. When sferics energy increases the number of associated sprites also increases. From the figure, it is seen that all the ELF sferics having energy greater than 12.5 dB are associated with sprites. Hence, high-energy ELF sferics could be considered as an indicator of sprites. Further, it is known that the measurement of sferics energy is easier as compared to measurement of weak signal of sprites. Reising *et al* [27] argued that the ELF sferics energy acts as a proxy indicator for the production of sprite if it exceeds 7 dB above the mean value. At a distance of ~500 km from sprite producing thunderstorm, they have been able to measure the second pulse of ELF sferics which is associated with about 20% of sprites. The simultaneity of the second ELF pulse with sprite luminosity indicates that the former is produced by currents in the body of the sprite [28]. Thus, measurements of the second ELF pulse can also be used to identify a relationship between sprite current and total sprite luminosity.

3. Sferics

Part of the VLF wave energy radiated during lightning discharge penetrate the atmosphere and propagate through the Earth-ionosphere wave-guide and is invariably recorded in the conjugate region along with whistlers as causative sferics. This propagation mechanism is known to contain information about the height of the reflecting layer and the travelling distance of the pulse. In the absence of appreciable dispersion, causative sferics appears as vertical traces on whistler sonograms except near the cut-off frequency of the wave-guide. The cumulative dispersion near the lower frequency end of the spectrum could be explained by

considering frequency dependent conductivity of the bounding surface (the Earth and the ionosphere). Further, it should be noted that the lower edge of the ionosphere is a diffused layer rather than a sharp reflecting layer. Outsu [30] has shown that the error introduced due to the assumption of perfect conductor for the reflecting layer in the travelling distance and reflecting layer height are 9% and 5% larger respectively. Reeve and Rycroft [31] recording tweeks during a solar eclipse deduced from the variation of the lower limiting frequency that the height of the lower ionosphere varied from 69 km to 76 km during the eclipse period. Barr [32] and Yamashita [33] discussed the formation of tweeks and evaluated various parameters such as the phase velocity, attenuation coefficient, polarization, mixing ratio and excitation factor. Prasad [34] has studied the role of the conductivity of ground and sea mixed path, forming the lower surface of the Earth-ionosphere wave-guide on the VLF wave propagation through the guide and has explained the formation of tweeks. Higher order harmonics along with fundamental modes have been experimentally observed [5,6,35] which are interpreted by considering VLF wave propagation through the Earth-ionosphere wave-guide.

Sferics is used to locate the lightning source. Using the Earth-ionosphere wave-guide mode propagation, the distance traveled by sferics from the source can be estimated by determining the time interval between two close frequency f_1 and f_2, and is given by [5]

$$D = |\delta t|(V_{g1}V_{g2})/|V_{g2} - V_{g1}|, \tag{1}$$

where V_{g1} and V_{g2} are group velocities of waves of the same mode determined at different frequencies f_1 and f_2 and δt is the time difference measured from spectrogram of tweeks between two chosen frequencies. Using the above formulation, Singh *et al* [5] estimated location of the source, which was not far from the recording site Varanasi. Further, the reflection height corresponding to the fundamental frequencies and the second and the third harmonics were estimated which lead to the conclusion that the upper boundary of the wave-guide is a diffused boundary.

The higher harmonics are used to estimate ionization density at the boundary of the wave-guide. From the Appleton-Hartree equation, the wave reflection condition, which is independent of direction of propagation, is given by

$$\omega_p^2 = \omega^2 + \omega\omega_H, \tag{2}$$

where ω_p is angular plasma frequency and ω_H is angular electron gyro-frequency. For VLF wave propagation, $\omega \ll \omega_H$ and from the reflection condition for the cut-off wave frequency $\omega = \omega_c$, the electron density is obtained as

$$N = 1.25\ \omega_c \times 10^{-8} f_c f_H\ \text{cm}^{-3}. \tag{3}$$

Near the lower edge of the ionosphere which is also the upper boundary of the wave-guide, $f_H \simeq 1.34$ MHz can be considered. Under this condition, the above equation reduces to

$$N = 1.66 \times 10^{-2} f_c\ \text{cm}^{-3}. \tag{4}$$

In the case of tweeks, f_c is the cut-off frequency of the tweeks. Shvets and Hayakawa [6] analyzed dynamic spectra of multi-mode (eight mode) tweeks shown in Figure 5. From the cut-off frequency of the mode, fundamental frequency for all the modes is found to be practically same. Using the trend of these values, if we estimate electron density, we find an increase in the electron density from 28 to 224 cm^{-3}, in the altitude range of 2 km at the height of 88 km.

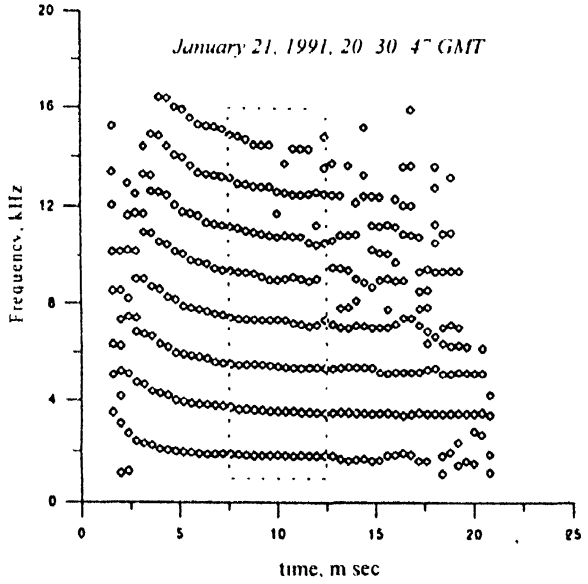

Figure 5. Extended dynamic spectrum of multimode tweek recorded on January 21, 1991 at 20 30 47 GMT. The cut-off frequencies are in the ratio 1 2 3 4 5 6 7 8 (after Shvets and Hayakawa, [6])

If the boundary walls of the wave-guide are not perfectly conducting surfaces, then the higher order modes are attenuated. The attenuation factor defined as the number of dB per 1000 km of path length is given by [5]

$$\alpha_n = 1.816 \times 10^{-1} f y_n, \tag{5}$$

$$y_n = -(n\pi/kh)(\Delta/n\pi)/X_n,$$

$$X_n = [(1 - n^2\pi^2/k^2h^2 + \Delta^2/n^2\pi^2)/2 + \{(1 - n^2\pi^2/k^2h^2 + \Delta^2/n^2\pi^2) + 4\Delta^2/k^2h^2\}^{1/2}/2]^{1/2},$$

$$\Delta = \mu_\omega(1/\mu_i + 1/\mu_g),$$

μ_i and μ_g are refractive indices of the ionosphere and the Earth-surface respectively. μ_ω is the refractive index of the material filling the wave-guide. Other parameters are defined by Singh *et al* [5]. The attenuation coefficient for different mode for the finite conductivity of the Earth-surface

(σ_e = 10^{-5} mho/m) and inner ionospheric layer (σ_i = 10^{-5} mho/m) is evaluated which is shown in Figure 6. The computation is made for wave-guide height h = 88, 92 and 96 km respectively. It is noted that the attenuation increases greatly as the frequency approaches the cut-off frequencies.

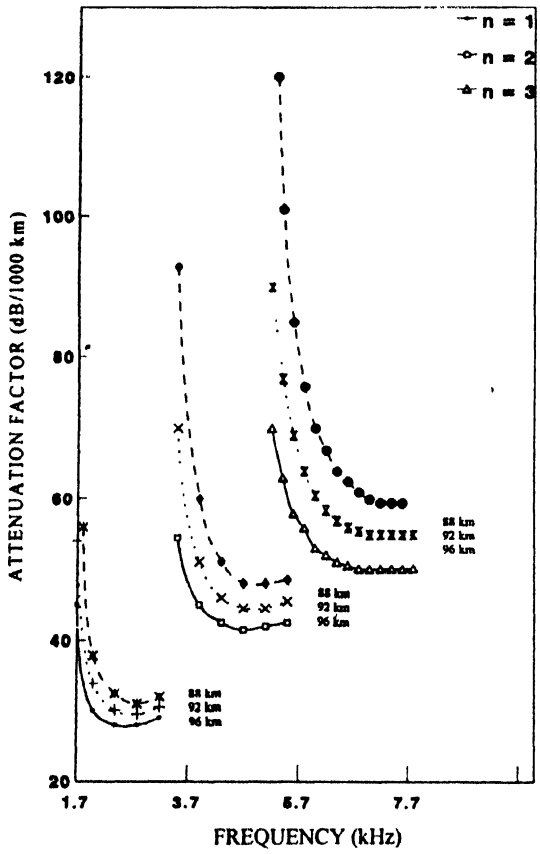

Figure 6. Wave attenuation as a function of frequency for the fundamental, the second and the third harmonics for waveguide height 88, 92 and 96 km respectively and σ_i = 10^{-4} mho m^{-1}, σ_E = 10^{-5} mho m^{-1}.

It also increases when the layer height decreases. This attenuation *versus* frequency characteristics explains the existence of lower limit of frequency of waves. Further, it is evident that as the waveguide mode number increases, attenuation increases. For example, the fundamental mode has approximately 30 dB/1000 km attenuation except near the cut-off frequencies. The second and the third harmonic modes have attenuation coefficients about 50 dB/1000 km and 60 dB/1000 km respectively. If the conductivity of anyone layer or both is increased then the attenuation factor is decreased. For a perfectly conducting waveguide layer $\Delta \rightarrow 0$, which shows that the attenuation factor for each mode vanishes and the fundamental tweeks alongwith its higher harmonics should be observed. However, in practice as the harmonic number increases its probability of observation decreases. The harmonic tweeks higher than the third have not been detected at Indian stations, although at high latitudes they have been observed [35].

The wave-guide mode theory is also used to reproduce theoretically the dynamic spectra of tweeks. For one set of conductivity the spectra of tweeks up to three modes are shown in Figure 7. It is found that as the height of wave-guide increases, the computed time delay decreases for a given frequency. Further, as the wave mode number increases the separation between spectrum increases. In the computation total path is taken as 2000 kms. If we consider finite conductivity of the Earth then dispersion near cut-off frequencies will be increased. If we consider diffused ionospheric layer, then dispersion will be enhanced. This is experimentally observed.

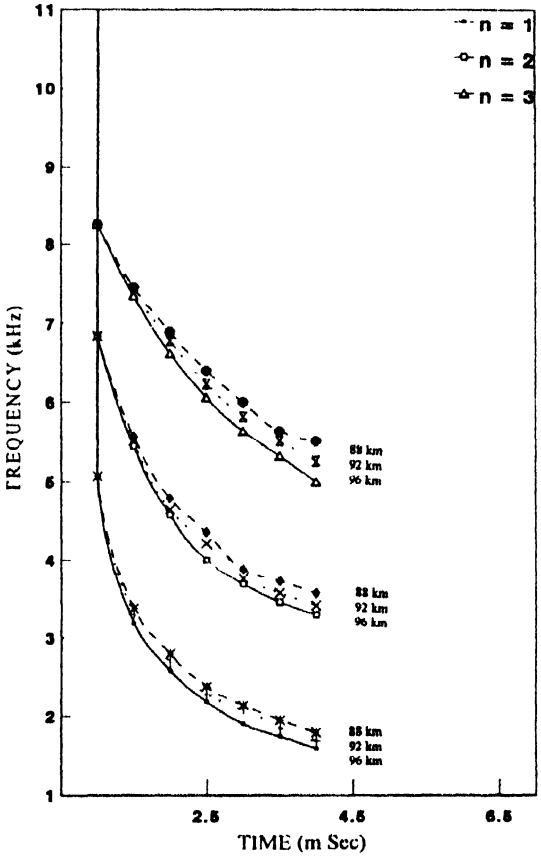

Figure 7. Computed frequency-time spectra of the fundamental, the second and the third harmonics for d = 2000 km σ_i = 10^{-4} mho m^{-1}, σ_E = ∞ mho m^{-1}.

Hayakawa *et al* [36] using sophisticated signal processing technique analyzed digital data of wave form and obtained frequency dependence of incident and azimuthal angles, and wave polarization of tweek sferics. The observed value of wave polarization can be a useful quantity to study the inhomogeneity and anisotropy of the lower ionosphere [36,37]. Rafalsky *et al* [38] have developed a new technique to estimate distance of the lighting discharge. In this method, the phase spectrum of the first mode of the Earth-ionosphere wave-guide is to be approximated with a model function of two main parameters : the ionospheric height and the

distance to the source, in the frequency range between the first and the second cut-off frequencies. The effectiveness of the technique was tested on a number of atmospherics from distant (900–3000 kms) sources. The discussions presented in this section clearly show that tweek sferics can be used to characterize the lightning discharge and the lower ionosphere.

4. Whistlers

Radiation in a relatively low frequency range (~ 0.3–30 kHz) during lightning discharge is the source of whistlers. After radiation from lightning discharges, the VLF waves penetrate the atmosphere, the ionosphere and get trapped in to the duct spread along the geomagnetic field lines. Dispersion is produced in the VLF wave energy during propagation, which causes the production of whistler waves. Thus, apart from the source effect, problems related with the transmission of waves through the ionosphere, wave trapping in the duct, wave leakage from the duct, existence of the ducts, *etc.* control the occurrence of whistlers. Whistlers propagate through the ionosphere and the magnetosphere in the whistler mode, which is possible only in the magnetized plasma and at frequencies below both the plasma frequency and electron gyro-frequency. The waves guided through the magnetosphere by field-aligned irregularities or ducts can propagate from one hemisphere to the other hemisphere without loss of energy and with appreciable dispersion. The reflection of wave energy either from the ground or from the ionosphere produces multi-hop spectrum of whistlers. Usually, a lightning discharge illuminates more than one duct in the magnetosphere and the resulting whistler trace consists of several discrete components separated in time due to differences in travel time through different ducts. Such whistlers are called multicomponent whistlers.

If a receiver is placed in space, onboard a satellite or a rocket, whistlers whose path deviate significantly from the Earth's magnetic field lines can also be detected. Such non-ducted whistlers show a wide variety of frequency-time signature depending on the location of the receiver, and on the electron density distribution and ion composition of the medium. Apart from the fact that the whistler dispersion is controlled by the electron and ion distributions of the ambient medium, there is also evidence that whistlers interact with energetic electrons present in the radiation belts during their transit through the magnetosphere. Such interactions may result in the amplification of the whistlers, triggering of emissions at new frequencies, and precipitation of some of the interacting energetic electrons [39,40]. Precipitating energetic electrons in turn produce enhanced ionization, heat, and optical emissions in the ionosphere, as well as X-rays detectable down to about 30 km altitude [41–43]. Strangeways [44] has studied lightning induced enhancements of *D*-region ionization and whistler ducts using 3-*D* magnetospheric ray-tracing program. He has shown that the enhancement of *D*-region ionization is over much wider region than the actual duct width in the interaction region. Savchenko and Vaisman [45] have shown that the VLF hiss bursts observed on the ground can be formed by refraction and scattering of the VLF waves in the ionosphere on irregularities generated during the precipitation of energetic electrons induced by whistlers.

4.1. Probing of medium by whistler waves

The waves propagating through the plasma medium get dispersed, high frequency precedes the low frequency, and the entire signal tone is called as whistlers. The analysis of whistler dispersion yields information about the medium parameters such as electron density, total electron content in a flux tube, electron temperature, magnetic field and large-scale convective electric fields present in the medium.

The estimation of parameters of the medium involves various assumptions about the wave propagation and about the medium. Some of these are :

(i) Whistler waves are assumed to propagate along geomagnetic fields either in ducted mode or in pro-longitudinal mode.

(ii) Wave normal angle is assumed to be zero.

(iii) Amplification/attenuation of the wave during propagation is not considered.

(iv) The group velocity is given by $d\omega/dk$.

(v) The plasma is cold and collisionless.

(vi) Geomagnetic field is dipolar throughout the region of whistler wave propagation.

The dynamic spectra of whistler waves can be classified as spectra containing

(a) both initiating sferics and nose frequency,

(b) nose frequency only,

(c) initiating sferics only,

(d) neither nose frequency nor initiating sferics.

The dynamic spectra of whistlers falling under the first category was initially exploited for diagnostics of magnetospheric parameters. For the rest of the other categories of whistlers, extrapolation method has been proposed from time to time. Both the traditional methods and their extrapolations have been discussed and reviewed [7,46]. In probing the medium, whistler wave is considered to propagate along the geomagnetic field line. Errors due to ignoring small deviations from strictly longitudinal propagation are

usually less than 1%. Using the group refractive index for whistler mode, expression for travel time is written as

$$t(f) = \int n_g/c\,ds$$
$$= 1/2c \int f_p(s)/\left[ff_H(s)\{1 - f/f_H(s)\}^3\right]^{1/2} ds. \quad (6)$$

The above equation can be integrated numerically if f_p and f_H are known along the path of propagation. To evaluate the above integral, various models for the magnetospheric electron density have been proposed from time to time. Diffusive equilibrium model which is the most widely used, is written as

$$N(s) = N_{eq} I(\phi) = N_{eq} \times \left[\sum_i \xi_{i_1} \exp(-z/H_i) / \sum_i \xi_{i_1} \exp(-z_{eq}/H_i)\right]^{1/2}, \quad (7)$$

where $z = r_1 - r_1^2/r - (\Omega^2/2g_1)(r^2\cos^2\varphi - r_1^2\cos^2\varphi_1)$ and $H_i = kT_{i1}/m_i g_1$,

k is the Boltzmann constant, T is the temperature, ξ is the fractional concentration of an ion species. The subscript i refers to i-th ion species, 1 refers to an arbitrary reference level, eq refers to the magnetic dipole equator. Ω is the angular velocity of the Earth's rotation (7.27×10^{-5} rad/sec) and g_1 is the acceleration due to gravity at the reference level. For numerical computation, the reference level is considered as 1000 km. For low latitudes, the reference level has been considered 400 km. Usually, T = 1000 k and an ionic composition of 90% O^+, 8% H^+ and 2% He^+ at the reference level have been considered. Substituting for the plasma model and dipolar magnetic field, the time delay can be written as

$$= R_E L f_{peq} f_{Heq}/cf^2 \int_{\varphi_1}^{\varphi} I(\phi)\left[1 + 3\sin^2\phi\right] \times \cos^4\phi / \left[(f_{Heq}/f)\{1 + 3\sin^2\phi\}^{1/2} - \cos^6\phi\right]^{3/2} d\phi. \quad (8)$$

The above equation is used to evaluate f_n (nose frequency) and t_n (travel time for nose frequency) for propagation through the magnetospheric paths only. Correction in travel time for propagation through the ionosphere and the Earth-ionosphere wave-guide is carriedout. The corrected values f_n and t_n are used to estimate the parameters. The empirical formulas relating f_n and t_n to the magnetospheric parameters are [47]

$$f_{Heq} = K f_n,$$
$$N_{eq} = K_{eq} f_n t_n^2/L^5, \quad (9)$$
$$N_T = K_T f_n t_n^2/L,$$
$$N_1 = K_1 f_n t_n^2/L^5.$$

From the equatorial electron gyro-frequency f_{Heq}, the L-value of the path is obtained ($L = (1.74 \times 10^5/f_{Heq})^{1/3}$). N_{eq} is the equatorial electron density, N_T is the total number of electron inside magnetic flux tube extending from the reference level to the equator and having 1 cm^2 cross sectional area at the reference level. N_1 is the electron density at the reference height. The quasi constants K vary slowly with L.

The electron density in the equatorial plane and distribution of electron density along geomagnetic field lines is determined. Analyzing whistlers recorded continuously at a station, temporal variation of electron density can also be studied. Such a study is possible only when the occurrence rate is high for long duration. The equatorial average electron density as a function of L-value derived from whistler data recorded at Varanasi during March, 1991 is shown in Figure 8. In the same figure, average electron density derived from whistlers recorded at Siple (June, 1973)

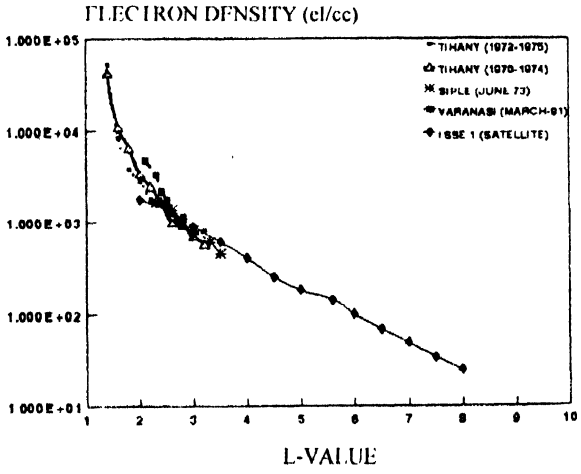

Figure 8. Variation of electron density as a function of L-value. Tihany (70-74) corresponds to winter period where as (72-75) corresponds to summer period For comparison purposes satellite (ISEE1) data is also included

and Tihani (1970-1974; 1972-1975) are also plotted. We find that our data compares well with those reported by others [48,49]. Tihani data were divided into summer (March-August, 1972-1975) and winter (October-February, 1970-1974) periods, It is seen that for $L > 2.4$, there is a lower density in summer than in the winter. In the same figure, we have plotted representative value of electron density profile for $2 < L \leq 8$ derived from ISEE1 satellite measurements. The measured profile belongs to very quite magnetic conditions and appeared to be well approximated by a linear relation between log N_{eq} and L-value. Carpenter and Anderson [50] have suggested that the derived plasmaspheric data in the L range $2 < L < 8$, can be represented by the empirical relation

$$N_{eq} = 10^{(-0.3145L + 3.9043)} el \text{ cm}^{-3}. \quad (10)$$

Similar expression was given by Park and Helliwell [48] where in the slope of the line, $d(\log Neq)/dL$ was -0.395 instead of -0.3145. The value obtained by Park and Helliwell [48] was based on plasmaspheric whistler data acquired under a wide range of magnetospheric conditions and hence it included the effects of disturbance-associated decreases in the outer plasmasphere. Errors introduced in the determination of N_{eq} values due to unavoidable approximations in the whistler analysis are discussed by Singh *et al* [7].

The remote sensing method discussed in this section using ground based facility does not yield local value of the electron density in the magnetosphere. Trakhtengerts and Rycroft [51] have suggested a method based on the phenomena of non-linear whistler wave reflection from the lower hybrid resonance level [52], which allows us not only to measure the local value of electron density but also to localize the place of measurements in the magnetosphere. Near the region of parametric reflection (when wave frequency becomes equal to lower hybrid resonance frequency), a sufficiently intense whistler signal generates two electrostatic plasma waves a resonance cone wave and an ion cyclotron wave. These two waves having minimal damping rate and minimal group velocity projections on to the magnetic field are effectively accumulated inside a narrow layer. This layer, filled by two plasma waves, serves as a non-linear mirror for the initial whistler wave. Using this new method, one can obtain important information about short scale low frequency turbulence (ion cyclotron waves) present in the magnetosphere [51].

The whistler technique is very useful in determining the location of plasma-pause and its movement during magnetic storm periods. Plasma-pause is the location at which density suddenly drops by an order of magnitude or more [53]. The density gradient at the plasmapause (in the equatorial region) were expected to be steepest and hence most readily identified in the hours following a sustained increase in magnetic disturbance activity. During recovery phase, refilling occurs and density gradients become less steep [50]. This has been established by whistler studies.

The total electron content in a flux tube of unit cross-section area at the reference height is obtained by evaluating the following integral

$$N_T = \int_{\text{ref}}^{\text{equator}} N(s)(B_r/B(s))\,ds, \qquad (11)$$

where B_r is the magnetic field at the reference height and $B(s)$ is the magnetic fields at any other point s along the field line. The above integral is evaluated and the variation of total electron content with L-value derived from whistler data is shown in Figure 9, which shows scattered behaviour. In spite of the rapid decrease in volume of geomagnetic field line tubes, the increase in N_T at lower L-value is unrealistic and can be explained by the electron density enhancement of the ducting structure above the ambient electron density.

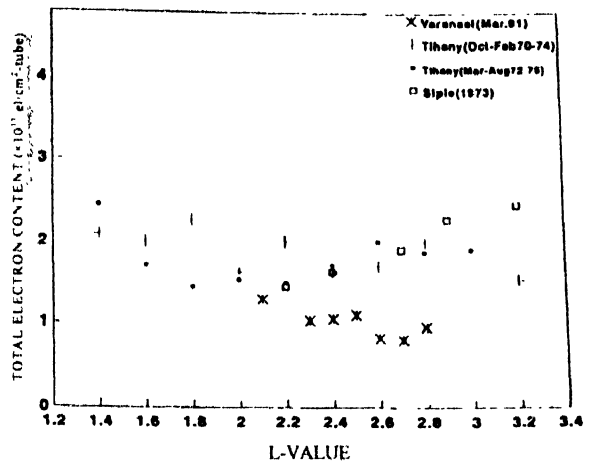

Figure 9. Variation of total electron content (electrons cm^{-2} tube $^{-1}$) in a flux tube with L-value is shown

At $L > 2$, density enhancements ~10% are sufficient to duct whistlers, where as at low L-values the enhancement factors ~100% are required for ducted propagation of whistlers. Hence, there is over estimation of electron density and total electron content in a flux tube derived from whistler data recorded at low latitudes.

The whistler technique has also been used to estimate the upward and downward transport of ionization flux which is found to be of the order of 10^9 electron/cm^2-sec. Singh *et al* [54] have argued on the basis of reported data that the downward transported flux increases with the increase in magnetic activity, which clearly supports that the large magnetic activity causes movement of plasma-pause closer to the surface of the Earth.

If a whistler duct drifts rapidly inward (outward), the nose frequency increases (decreases) with time. Such a drift is caused by an electric field. Drift velocity is given by $\boldsymbol{E} \times \boldsymbol{B}/B^2$. In the equatorial plane, it is given by $V_d = E/B$, where E is the east-west electric field. Comparing this drift velocity with the dirft velocity derived from whistler path deviation, electric field is estimated. If a large number of whistlers are analyzed then E can be determined with a precision of 0.1 mV/m. The technique has been widely used to measure east-west electric field during quiet times as well as storm times. Typically, the value is found to range between 0.1 and 0.7 mV/m [7].

Considering the upper cut-off frequency of the nose whistler to be due to thermal attenuation, the electron temperature has been estimated to vary between 1.7 eV

(2×10^6 K) and 4 eV at $L = 4$. The method was not widely used because it is difficult to distinguish whether the upper cut-off in the spectrum was due to thermal attenuation or propagational effects [55]. Attempt has also been made to infer magnetospheric electron temperature from whistler dispersion measurement [56].

The diffused nature of whistler trace yields information about duct width. Duct lifetime is determined from the power spectrum analysis of whistler data. Duct width may vary between 10 and 100 km. Duct life time usually varies between 30 minutes and 2 hours, although, duct life time as high as 1–2 days are also reported [7]. Ducts occupy relatively small volume (0.01%) in the magnetosphere. Cole [57] for the first time suggested the formation of field aligned ducts by interchange of plasma in flux tubes driven by $E \times B$ force. Park and Helliwell [58] suggested that the electric field E driving the plasma mixing in the flux tube is thundercloud electrostatic fields. Park and Dejnakarintra [59] computed high altitude electric fields due to electrified clouds taking in to account the presence of ionosphere and showed that the flux interchange mechanism of duct formation is plausible. The estimation of high altitude electric fields is highly sensitive to the atmospheric conductivity profile. Rodger *et al* [60] have shown that under 'typical' conductivity conditions the high altitude electric fields from even giant thunder clouds are too small to create a realistic whistler duct in a realistic period. This is valid for both day and night conditions.

The normal spectrogram of a whistler when analyzed by matched filtering technique produces a dynamic spectra with higher resolution in both frequency and time, and usually many fine structure component are seen [8,61,62]. These results indicate the existence of a number of fine structure ducts within a broader duct. Ray tracing computation showed that the rays first trapped in the main duct at low altitude may be further trapped within fine structure enhancements at higher altitudes. The exit from duct takes place in the reverse order [63]. The fine structure components are useful in probing the duct structure present in the magnetosphere and in understanding the ducted mode propagation of whistlers. Singh *et al* [64] and Singh and Hayakawa [65] have reported whistler triplets. Frequency and temporal fine-structure reported by them are individual whistlers having different dispersion and path of propagation, and hence fine structures reported by Singh and Hayakawa [65] are different than those reported by Singh *et al* [8,62]. Trace splitting of whistlers [8,61] can be explained by considering multimode propagation through the duct, as Laird [66] has shown that differences in propagation time between modes for ducted whistler paths can be of the order of millisecond. Further, duct clusters containing a large number of closely spaced ducts are not reported from satellite observations.

4 2. Earth quakes and whistler wave activity :

Both precursory and post-seismic variations in wide band ELF/VLF (from few Hz to few kHz) amplitudes are observed when the satellite passes over the active Earthquake zone [67,68]. The associated wave phenomena can be discussed in terms of generation of waves due to seismic changes and modification of wave amplitude/phase when the path of propagating wave from source to receiving point passes over the active Earthquake zone. All these observations considered together could lead to a possible understanding of wave phenomena associated with Earthquakes.

Recent observations ([69] and references there in) indicate wide frequency range electromagnetic wave association with Earthquake. There are two main hypothesis regarding the generation mechanism of these waves : (a) electromagnetic waves are directly emitted from the Earthquake focal region, (b) the emission is a result of electric charge redistribution in the Earth's atmosphere.

It is known that micro-fracture of the rock under the ground, continuously occurs before an Earthquake shock. The rocks under mechanical stress emit electromagnetic waves. This has been observed during laboratory experiments [70,71]. The strains or break down on the rock cause huge amount of the emission of the exo-electrons (free electrons). These electrons excite plasmons at frequency ($\omega_p = (ne^2/\varepsilon_r\varepsilon_0)^{1/2}$) which depends on the valance electron density and relative dielectric constant. Inside the Earth, n may vary between 10^{10}–10^{20} m^{-3} and ε_r lies in the range 3–10^2. The corresponding plasma frequency $f_p \sim (10^4$–$10^8)$ Hz. The plasma oscillations may be converted in to electromagnetic waves of the same frequency. Thus, the wave from 10 kHz onwards can be explained by this mechanism [72]. Although, the conversion process and propagation of the wave from the Earthquake focus to the atmosphere is not understood.

The plasma decay process proposed for high frequency waves can not explain the observed low frequency components. Kamogawa and Ohtsuki [73] proposed another model based on image-charge of the exo-electrons produced during rock fracturing. The exo-electrons regarded as free electrons continuously escapes from the stress area leaving behind positive charged region. Thus, we can assume that positive true charge exists. When the length between the charged area and the Earth surface is less than the Debye length, then an image charge appears inside the Earth. The existence of image charge can be understood by considering a parallel situation in solid state physics. If a charged area appears inside a metal at a distance smaller than the Thomas-Fermi length from the metal surface then because of the

inhomogeneous electric field screening, an image charge area is created inside the bulk. The Thomas-Fermi length λ_{TF} $V_f/\sqrt{3}\,\omega_p$, where Fermi velocity $V_f = (2E_f/m)^{1/2}$. E_f is the Fermi energy. Note that Thomas-Fermi length is based on the Fermi-Dirac distribution function. In the case of plasma, charged particles obey Boltzmann distribution function and hence λ_{TF} is replaced by λ_D. Assuming $T = 10^3$k, $n = 10^3$–10^{19} m^{-3}, $\varepsilon_r < 10^4$, $\lambda_D \sim 10^4$ m. This shows that for the usual Earthquake the length between the charged area to the Earth surface is shorter than the Deybe-length and the image charge can be considered to be inside the Earth. The motion of image charge produces the electromagnetic wave due to Bremsstrahlung mechanism. The motion of image charge, which is caused by the break down velocity of the rock; can explain the lower/very lower frequency components of the waves. The intensity and angular distribution can be studied by using standard formula for Bremsstrahlung radiation [74]. If the break down speed is of the order of 1 km/sec, the electromagnetic wave frequency is of the order of 10^3 Hz [73], which corresponds to the observation of the lower frequency component of the wave spectrum associated with Earthquake.

In another approach, the VLF waves may originate through the process of electric charge redistribution in the Earth's atmosphere causing electron density changes [68] or wave particle interaction in the ionosphere [75]. The linear polarization of the magnetic signals of the present VLF data as found in the satellite data also supports the idea that the VLF waves are generated in the secondary processes in the ionosphere rather than direct wave propagation from the epicenter of the Earthquake. For wave-particle interaction to take place, the wave must penetrate into the ionosphere without much attenuation. Hence, the wave must be very low frequency ($f << 1$ khz) wave. ELF waves of 225 Hz is observed to increase in amplitude much before than moderate Earthquake [76]. It is also possible that seismogenic oscillations of the lower ionosphere boundary and related VLF signal characteristics are induced by resonant gravity waves generated during the process of Earthquake preparation and relaxation [77]. These resonant atmospheric oscillations might be amplified at height of 70–90 km due to a non-equilibrium situation connected with strong winds present in the atmosphere.

The ionospheric perturbation caused by Earthquakes can be studied using the following four roots :

(a) The Earth's eigen oscillations are enhanced during Earthquake preparatory stage and generate internal gravity waves which may propagate through the atmosphere *via* acoustic mode and modify the parameters of the ionosphere.

(b) Deformation and fracturing of ground materials cause the generation of VLF/ELF electric currents. These currents generate electromagnetic emissions, which may penetrate into the ionosphere and be detected onboard satellites.

(c) During the preparatory stage of Earthquake radioactive gases (radons) emanate and affect the air conductivity. Hence, fair-weather current enhances and additional joule heating of the lower ionosphere modifies (slightly) the ionospheric parameters.

(d) The variations in near Earth electrostatic field, generation of internal gravity waves and other kinds of seismogenic effects may change the photochemical equilibrium of the ionosphere. Thus, the diffusion process in the upper atmosphere is modified.

The continuous monitoring of VLF wave amplitude and phase show that the wave phase and amplitude change before the Earthquake, if the path of propagation from transmitter to the receiving system passes over the active Earthquake zone. These changes may be due to changes in the ionization density of the lower ionosphere, which effectively changes the height of Earth-ionosphere wave-guide. In fact the excess ionization caused by seismic effects reduces the height of Earth-ionosphere wave-guide. Some observations are reported which support this view, but further study in this area is required.

ELF/VLF electromagnetic effects associated with seismic activity are a relatively new research area. The associated observation and their interpretation are at the premitive stage. A comprehensive study, making use of adequate data analysis and comparison and taking in to account all known physical causes of ELF/VLF emissions, would add immensely to this field. It has been observed that different techniques used for observation and classification of seismo-active increases have yielded conclusions differing from one another [78]. It is not clear whether the methods employed are responsible for such differences or the existence of effect is doubtful. Therefore, in order to establish the properties and dependencies of this phenomena, more than one method should be applied to a large data set of events. The geological dependencies of the reported seismo-electromagnetic activity should be explored. The role/effects of faulty systems, surface conductivities, characteristics of the shock's (magnitude, depth, sea/land), and whether the earthquake occurs on a tectonic plate boundary, on the observability of 'seismo-active' increases have to be studied before constructing an accurate physical model for the remote sensing and forecasting of earthquake.

5. VLF waves and optical waves

The observations of optical waves in recent years associated with lightning discharges, have completely changed the perception of the region above the thunderstorm. The region was previously considered to be passive with a limited role in allowing the passage of vertical current to maintain the electrification of the fair weather atmosphere and radio waves to the ionosphere The chance observation of optical emissions in this passive region has revolutionized the study of thunderstorm activity and its effect. The optical emissions include red sprite, blue jets, blue starters and elves; all in the wave length region 600-800 nm. Red sprites are bright channels extending vertically up from 40 kms to > 90 kms having variable width and shape. Depending on the shape of the column, they are termed as jellyfish, plumes, carrots *etc*. They develop to full brightness in 1–3 ms and may last for 10–100 ms [79]. Recent measurements of the spectrum of sprites show it to be the first positive N_2 band as that observed in Geisslertube discharge of air at a pressure of 0.2 to 2 mm [80], which corresponds to pressure in the atmosphere of 40–65 km. This suggests that red sprites could be the positive column of a cloud-ionosphere discharge. Dowden *et al* [81] suggested that sprites could be triggered by a meteor or cosmic ray shower after a cloud-to-ground discharge had set up a static electric field. Sprites could also be triggered by whistler induced electron precipitation [82].

Elves (emission of light and VLF perturbation from electromagnetic pulse sources) are bright but diffuse luminous disks formed by the electromagnetic pulse of the cloud to ground lightning discharge, which produces both light and ionization [83]. Despite the very brief life of the light (about 1 ms), the ionization so produced decays, as does the sprite, by the processes and in times (~1 to 100 s) determined by the chemistry, collision frequency, *etc*. appropriate to the altitude (75–105 km). The horizontal width of elves is about 100–300 km. The very rapid (3.1 + 0.8 times the speed of light) horizontal expansion of elves supports the view that it is due to an electromagnetic pulse creation mechanism.

Blue jets are deep blue in appearance and the emission is assumed to be the first negative group system of N_2^+. They propagate upward starting from small regions directly above the active core of thundercloud with a speed of 75–220 km/sec. The terminal altitude reached is 40–50 km. Blue jets are longer lived than red sprites and have a life time of about 250 ms, with the brightness decaying simultaneously along its length. Blue starters are distinguished from blue jets by their much lower terminal altitude (~25 km) and they are brighter than blue jets. The emission profile has not yet been measured but it is assumed to be from the first negative band of N_2^+.

The VLF wave (whistlers and emissions) propagating through the magnetosphere interacts with electrons and causes their precipitation, which in turn modify the Earth-ionosphere wave-guide. The precipitated electrons interact with the VLF waves propagating through the Earth-ionosphere wave-guide and modify the amplitude and phase of the interacting wave. These were first observed by Trimpi in Antarctica on the VLF transmissions from NSS (Annapolis, Maryland) and NAA (Cutler, Maine) [84]. These perturbations were associated with whistlers and the delay in the onset of Trimpi was of the order of minutes. Armstrong [41] reported rapid-onset of Trimpi with essentially no delay (< 50 ms) from the initiating lightning, and hence, precluded whistler-induced electron precipitation as the cause, because this takes longer times. The Trimpi having rapid-onset also decayed rapidly and can occur with or without accompanying whistler induced electron precipitation. The perturbation of phase and amplitude of VLF waves could also be produced by sprites and elves. These are called either as VLF sprites or VLF elves. A schematic arrangement is shown in Figure 10. In the figure it is suggested that the optical emissions (sprites/elves/blue jects) are associated with the

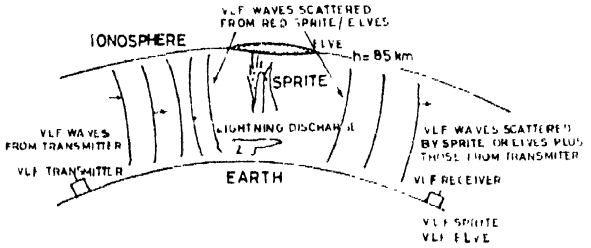

Figure 10. Schematic diagram showing VLF wave perturbation caused by red sprite and production of VLF sprite.

production of ionization which causes Trimpi on the VLF waves from a transmitter propagating through the Earth-ionosphere wave-guide. The amplitude and phase perturbations of the VLF waves can be measured at the receiving sites. VLF sprites have an identifiable time signature, they decay logarithmically with time, not exponentially as is expected in the previous case and also is observed for classic Trimpi [85]. The logarithmic decay are explained in terms of scattering from a vertical column or number of columns extending from ≤ 50 km to ~80 km altitude [81].

The above discussion clearly shows that the VLF sprites can be used to study the electrical properties of the red sprite plasma. Rodger *et al* [86] examined the scattering of VLF waves by a finite-length column of ionization inside the Earth-ionosphere wave-guide including the effect of curvature

of the wave-guide. Some sample calculations show the detectability of red sprite at long distances (~2000 m) which otherwise could not be observed. Thus, it is shown that VLF waves can be used to probe the optical emissions at large distances, which are not possible by direct measurements.

6. Conclusions

In this review, an attempt has been made to discuss the features of waves associated with lightning discharges, and their diagnostic feasibility. We have considered ELF and VLF waves along with optical emissions. We have also discussed the effect of Earthquake on the generation and propagation of ELF/VLF waves. From the present study, following points emerge :

(i) The energy of the Earth-ionosphere cavity resonance is a good indicator of transient optical emissions observed above the thunderstorms.

(ii) High energy ELF sferics (energy > 12.5 dB) could be considered as an indicator of red sprite The second ELF pulse quantifies relationship between sprite current and total sprite luminosity.

(iii) VLF sferics (tweeks) can be used to locate the lightning source and to estimate electron density at the inner edge of the ionosphere.

(iv) Dispersion produced in the dynamic spectra of sferics near the wave-guide mode cutoff frequencies is a function of conductivity of the Earth and the ionosphere and hence information about the conductivity of the system can be derived

(v) Whistler waves are used to estimate the equatorial electron density, electron density along the path of propagation and total electron content in a flux tube The large scale convective electric field, duct width and duct life times are also evaluated from the dispersion analysis of whistlers with reasonable accuracy

(vi) It is found that whistlers recorded at Varanasi are part of mid-latitude whistlers and they have propagated to low latitude ground station through the Earth-ionosphere wave-guide Recording whistlers at low latitudes, mid latitude magnetosphere can be probed.

(vii) Ground based and satellite observations indicate wide frequency range electromagnetic wave association with Earthquake. The observation may be explained in terms of generation of waves due to seismic changes and modification of wave amplitude and phase when the path of propagating VLF wave from source to receiving point passes over the active Earthquake zone.

(viii) As in the case of Trimpi effects, the ionization associated with optical emissions can perturb the amplitude and phase of the propagating VLF wave. Perturbation will be of short duration and hence the monitoring of amplitude and phase of the VLF waves transmitted from a station will provide information about the optical emissions. Schematic arrangement has been proposed to study this effect

Acknowledgment

The work is supported by the Department of Science & Technology, Government of India under SERC project. We are thankful to the referee for his suggestions and critical remarks.

References

[1] G J Fishman, P N Bhat, R Mallozzi, J M Horack, T Koshut C Kouveliotou, G N Pendleton, C A Meegan, R B Wilson W S Paciesas, S J Goodman and H J Christian *Science* **264** 1313 (1994)

[2] C J Rodger *Rev. Geophys* **37** 317 (1999)

[3] G Milikh and J A Valdivia *Geophys. Res. Lett* **26(4)** 525 (1999)

[4] D D Sentmann, F M Wescott D L Osborne, D L Hampton and M J Heavner *Geophys. Res. Lett* **22** 1205 (1995)

[5] R N Singh, R P Singh, U P Singh and A K Singh *Indian J. Radio Space Phys* **21** 377 (1992)

[6] A V Shvets and M Hayakawa *J. Atmos. Solar Terr. Phys* **60** 461 (1998)

[7] R P Singh, Ashok K Singh and D K Singh *J. Atmos. Solar Terr. Phys* **60** 495 (1998)

[8] R P Singh D K Singh A K Singh D Hamar and J Lichtenberger *J. Atmos. Solar Terr. Phys* **61** 1081 (1999)

[9] J Bosokova and K Jiricek *Studia Geophys. Et Geod* **30** 196 (1986)

[10] G P Chernov *Solar Phys* **130** 75 (1990)

[11] I Nagano, X Y Wu, S Yagitani and K Miyamura *J. Geophys. Res* **103** 11827 (1998)

[12] Y Hobara, O A Molchanov, M Hayakawa and K Ohta *J. Geophys. Res* **100** 23523 (1995)

[13] D A Gurnett, W S Kurth, I H Cairns and L J Granroth *J. Geophys. Res* **95** 20967 (1990)

[14] D A Gurnett and W S Kurth in *Neptune and Triston* (ed) D P Cruikshankkl (Tucson Univ of Ariz Press) p389 (1995)

[15] J L Scarf *Adv. Space Res* **5** 31 (1985)

[16] K D Cole and W R Hoegy *J. Geophys. Res* **102** 14615 (1997)

[17] R J Strangeway *J. Geophys. Res* **102** 11665 (1997)

[18] M Cho and M J Rycroft *J. Atmos. Solar Terr. Phys* **60** 871 (1998)

[19] D L I Jones *New Sci* July 4 **37** (1985)

[20] E R Williams *Science* **256** 1184 (1992)

[21] W O Schumann *Z. Naturforsch* **7a** 149 (1952)

[22] M A Uman *International Geophysical Series* (Orlando, FL Academic) **39** (1987)

[23] D D Sentmann *Atmospheric Electricity* (Boca Raton FL CRC Press) **1** 267 (1995)

[24] A P Nickolaenko, L Ranbinowicz and M Hayakawa *J. Atmos. Electricity* **18** 1 (1998)

[25] A P Nickolaenko, M Hayakawa and Y Hobora *J Geophys Res* **104** 27785 (1999)

[26] M Abbas *Planet Space Sci* **16** 831 (1968)

[27] S C Reising, S I Umran and F B Timothy *Geophys Res Lett* **26** 987 (1999)

[28] S A Cummer, U S Inan, T F Bell and C P Barrington-Leigh *Geophys Res Lett* **25** 1281 (1998)

[29] M Fullekrug and S C Reising *Geophys Res Lett* **25** 4145 (1998)

[30] J Outsu *Proc Res. Inst Atmos* (Nagoya University) 7 58 (1960)

[31] C D Reev and M J Rycroft *J Atmos. Terr. Phys.* **34** 667 (1972)

[32] R Barr *ELF-VLF Radio Wave Propagation* (ed) J A Holtel (Dardrecht, Holland . D Reidel) p225 (1974)

[33] M Yamashita *J Atmos Terr Phys* **40** 151 (1978)

[34] R Prasad *J Atmos Terr Phys* **43** 1271 (19810

[35] R A Helliwell *Whistlers and Related Ionospheric Phenomena* (Stanford Stanford University Press) (1965)

[36] M Hayakawa, K Ohta, S Shimakura and K Baba *J. Atmos Solar Terr Phys.* **57** 467 (1995)

[37] M Hayakawa, K Baba and K Ohta *J Geophys Res* **99** 10733 (1994)

[38] V A Rafalsky, A V Shvets and M Hayakawa *J Atmos Solar Terr Phys* **57** 1255 (1995)

[39] M J Rycraft *Planet Space Sci* **21** 239 (1973)

[40] B T Tsurutani and G S Lakhina *Rev Geophys* **35** 491 (1997)

[41] W C Armstrong *Antarctic J. USA* **18** 281 (1983)

[42] W J Burke *J Atmos Terr Phys* **54** 205 (1992)

[43] U S Inan, J V Rodriguez and V P Idone *Geophys Res Lett* **20** 2355 (1993)

[44] H J Strangeways *J Atmos Solar Terr Phys.* **61** 1067 (1999)

[45] P P Savchenko and G M Vaisman *Geomagn. Aeron* **39** 99 (1999)

[46] S S Sazhin, M Hayakawa and K Bullough *Ann Geophys* **10** 293 (1992)

[47] C G Park *Tech Report 3454-1* (Radio Sciecne Lab. Stranford University, USA) (1972)

[48] C G Park, D L Carpenter and D B Wiggin *J Geophys Res.* **83** 20967 (1978)

[49] G Tarcsai, P Szemeredy and L Hegymegi *J Atmos. Terr Phys.* **50** 607 (1988)

[50] D L Carpenter and R R Anderson *J Geophys. Res.* **97** 1097 (1992)

[51] V Y Trakhtengerts and M J Rycroft *J Atmos. Solar Terr. Phys.* **60** 545 (1998)

[52] V Y Trakhtengerts, M J Rycroft and A G Demekhov *J. Geophys Res.* **101** 13293 (1996)

[53] D L Carpenter *J. Geophys. Res* **71** 693 (1966)

[54] R P Singh, Lalmani and U P Singh *Ann. Geophys.* **11** 1011 (1993)

[55] S S Sazhin, A J Smith and E M Sazhin *Ann. Geophys.* **8** 273 (1990)

[56] S S Sazhin, P Bognar, A J Smith and Gy Tarcsai *Ann. Geophys* **11** 619 (1993)

[57] K D Cole *J. Atmos. Terr. Phys.* **33** 741 (1971)

[58] C G Parkand and R A Helliwell *Radio Sci.* **6** 299 (1971)

[59] C G Park and M Dejnakarintra *J Geophys. Res.* **78** 6623 (1973)

[60] C J Rodger, N R Thomson and R L Dowden *J. Geophys Res* **103** 2171 (1998)

[61] D Hamar, C Ferencz, J Lichtenberger, G Tarcsai, A J Smith and K H Yearby *Radio Sci* **27** 341 (1992)

[62] R P Singh, R P Patel, Ashok K Singh, D Hamar and J Lichtenberger *Pramana-J Phys* **55** 685 (2000)

[63] H J Strangeways *J Atmos Solar Terr Phys* **44** 901 (1982)

[64] B Singh, R Singh and R Singh *Geophys Res Lett* **24** 2507 (1997)

[65] B Singh and M Hayakawa *J Atmos Solar Terr Phys* **63** 1133 (2001)

[66] M J Laird *J Atmos Solar Terr Phys* **54** 1599 (1992)

[67] M B Gokhberg, V A Morgounov, T Yashino and I Tomizawa *J Geophys Res* **87** 7824 (1982)

[68] M Parrot, F Lefeuvre, Y Corcuff and P Godefroy *Ann Geophys* **3** 731 (1985)

[69] M Hayakawa *Atmospheric and Ionospheric Electromagnetic Phenomena Associated with Earthquake* (Japan Terra Scientific) (1999)

[70] V Nitsan *Geophys Res Lett* **4** 333 (1977)

[71] Y Enomoto and H Hashimoto *Nature* **346** 641 (1990)

[72] Y H Ohtsuki and M Kamogawa *Plasmon-decay model for origin of EMW noises in the Earthquakes* (ed) M Hayakawa (Japan Terra Scientific Publications) p 395 (1999)

[73] M Kamogawa and Y H Ohtsuki in *Image charge model for origin of EMW noises in the Earthquake* (ed) M Hayakawa (Japan Terra Scientific) p 401 (1999)

[74] J D Jackson *Classical Electrodynamics* (New York Wiley) (1975)

[75] O A Molchanov, O A Mazhaeva, A N Goliavin and M Hayakawa *Ann Geophys* **11** 431 (1993)

[76] M Hata, X Tian, I Takuni, S Yabashi and A Imaizumi *J Atmos Electr* **16** 199 (1996)

[77] O A Molchanov and M Hayakawa *J. Geophys Res.* **103** 17489 (1998)

[78] C J Rodger, R L Dowden and N R Thomson in *Atmospheric and Ionospheric Electromagnetic Phenomena Associated with Earthquakes* (ed) M Hayakawa (Tokyo . Terra Scientific) p697 (1999)

[79] J R Winckler, W A Lyons, T F Nelson and R J Nemzek *J Geophys Res.* **101** 6997 (1996)

[80] S B Mende, R L Rairden, G R Swenson and W A Lyons *Geophys Res. Lett.* **22** 2633 (1995)

[81] R L Dowden, J Brundell, C Rodger, O Molchanov, W Lyons and T Nelson *IEEE Antenna and Propagation* **38** 7 (1996)

[82] W K M Rice and A R W Hughes *J Atmos. Solar Terr Phys* **60** 1149 (1998)

[83] Y N Taranenko, U S Inan and T F Bell *Geophys Res Lett* **20** 6527 (1993)

[84] R A Helliwell, J P Katsufrakis and M L Trimpi *J Geophys Res* **78** 4679 (1973)

[85] R L Dowden, J B Brundell and C J Rodger *Geophys Res Lett* **24(19)** 2419 (1997)

[86] C J Rodger, N R Thomson and J R Wait *Radio Sic* **34** 913 (1999)

About the Reviewers

Prof. R P Singh, born in 1943, received his education at Banaras Hindu University. Currently he is Professor in the Physics Department, Banaras Hindu University, Varanasi. After getting PhD degree in 1969, he has worked at the leading Space Physics Laboratory in Paris, France from 1970 to 1973. Professor Singh has visited USA, UK, Germany, Italy, Belgium, France, Holland and Hungary and has delivered lectures in leading laboratories of the above countries. Professor Singh has collaborative projects with Indian and foreign scientists. He has published more than hundred papers in the International Journals. The current research interest of Professor Singh is waves in space plasma, space weather and polymer physics.

R P Patel, born in 1971, received his education at Purvanchal University and is working for PhD degree at the Physics Department, Banaras Hindu University. He participated in the 20th Indian Antarctic Scientific Expedition during December 2000 to April 2001. The field of interest is ELF/VLF/VHF waves in Space Plasma.

Dr. Ashok K Singh, born in 1964, received his education from Banaras Hindu University and obtained his PhD in 1995 in magnetospheric studies using whistlers. After doctoral work, he was awarded Research Associateship from Council of Scientific and Industrial Research (CSIR). After completing the project he worked in space plasma division at Indian Institute of Geomagnetism, Mumbai on computer simulation of geotail dynamics. Dr. Singh has worked at Geophysical Department, Eotvos University, Budapest, Hungary as a visiting scientist. Presently, he is working in the field of magnetospheric physics and space weather predictions.

Dr. I M L Das, born at Darbhanga, Bihar, obtained his higher education from Banaras Hindu University. Currently, he is a reader in the Physics Department, Allahabad University, Allahabad. He got his PhD from Banaras Hindu University in 1981 in Space Plasma Physics. He has published a large number of papers in International Journal. Presently, his interest is in ionosphere phenomena and space plasma physics.